Clays and Clay Minerals (2024), **72**, e13, 1–14
doi:10.1017/cmn.2024.18

Original Paper

Influence of mineral composition and firing temperature on the micro- and mesoporosity of replicate archaeological ceramics

Jan-Michael C. Cayme[1], Rasmus Palm[1,2], Peeter Somelar[3], Signe Vahur[1], Ivo Leito[1] and Ester Oras[1,4,5]

[1]Institute of Chemistry, University of Tartu, Ravila 14A, Tartu, Estonia; [2]Department of Applied Physics, KTH Royal Institute of Technology, Stockholm, Sweden; [3]Department of Geology, University of Tartu, Ravila 14A, Tartu, Estonia; [4]Department of Archaeology, University of Tartu, Jakobi 2, Tartu, Estonia and [5]Swedish Collegium for Advanced Study (SCAS), Linneanum, Thunbergsvägen 2, Uppsala, Sweden

Abstract

The role of micro- and mesopores of archaeological ceramics in preserving ancient biomolecules is not well established. To understand the formation of these nano-sized pores in ceramics, reference pottery briquettes were made using two different clay types (illitic and kaolinitic clays), two different tempers (sand and chalk), and two different firing temperatures (600 and 800°C). The mineral content of the briquettes was determined by quantitative X-ray diffraction, and the micro- and mesopores were characterized with the N_2 adsorption method. The Brunauer–Emmett–Teller method, the adsorbed volume near liquefaction, and application of non-local density functional theory (NLDFT) were used on the N_2 adsorption data to determine specific surface areas, specific pore volumes, and pore-size distributions. Values of the micro- and mesoporosity parameters of most of the briquettes were approximately proportional to the initial clay content and unrelated to temper; the proportionality factors were much larger for illitic clay than for kaolinitic clay. When chalk-tempered briquettes were fired at the higher firing temperature of 800°C, the parameters were no longer proportional to the initial clay content; they decreased in most briquettes formed of illitic clay due to reaction of the clay with lime, and they increased in briquettes formed of kaolinitic clay due mostly to the porosity of unreacted lime. Micropore volumes in briquettes formed mostly of illitic clay were substantial: of the order of 5 $mm^3\ g^{-1}$. The work presented here forms a basis for future studies to establish a plausible mechanism of organic residue absorption and preservation in ancient ceramics.

Keywords: clay; ceramics; porosity; N_2 adsorption; X-ray diffraction

(Received: 18 February 2024; revised: 14 April 2024; accepted: 18 April 2024)

Introduction

Archaeological ceramics are valuable heritage objects that document and describe very different aspects of past material culture. Investigation of archaeological ceramics gives insight into manufacturing traditions, raw material availabilities, and technological preferences, as well as artistic expressions of past communities. Ancient ceramics were molded from clays and non-clay materials and fired at an elevated temperature (Orton and Hughes, 2013). Tempers were usually added to prevent shrinking and cracking during the firing process. The tempers ranged from mineral inclusions, such as crushed rocks and shells, to organic materials, like hair and plant remains, and previously fired clay substances (grog or chamotte) (Santacreu, 2014). Firing was done in either an oxidizing or a reducing environment, and with variable heating rates and soaking times, and it is known that firing conditions affect the degree of alteration of the microstructure and mineralogical composition of clay ceramics (Seetha and Velraj, 2015; Daghmehchi et al., 2018; Mentesana et al., 2019). All these different materials and manufacturing procedures influenced the physical characteristics of archaeological ceramics, such as strength, hardness, density, and porosity.

Although the range of archaeological clay artifacts varies from figurines and mundane utensils (e.g. spindle whorls) to building materials (e.g. bricks and clay daubs), the vast majority of archaeological clay objects are fragmented pottery. Besides the traditional typo-chronological value of ancient pottery, studies in recent decades have proven that it is a valuable source of information in decoding ancient diet, contributing to the understanding of not only food but also the economy, ways of life and environmental circumstances in the past (Roffet-Salque et al., 2015; Oras et al., 2017; Lucquin et al., 2018; Courel et al., 2020; Evershed et al., 2022). This knowledge is achieved through organic residue analysis, which relies on the extraction and identification of absorbed organic compounds, mostly lipid components, from pottery samples (Evershed et al., 2002; Evershed, 2008a; Roffet-Salque et al., 2017).

While the preservation of original lipid components coming from food residues in archaeological pottery is widely proven, the mechanism of retention of organic molecules within the inorganic

Corresponding author: Jan-Michael C. Cayme; Email: jan-michael.cayme@ut.ee
Cite this article: Cayme J.-M.C., Palm R., Somelar P., Vahur S., Leito I., & Oras E. (2024). Influence of mineral composition and firing temperature on the micro- and mesoporosity of replicate archaeological ceramics. *Clays and Clay Minerals* **72**, e13, 1–14. https://doi.org/10.1017/cmn.2024.18

structure of the ceramic vessels is still poorly known (Hammann et al., 2020). Understanding how the physicochemical properties of the pottery materials are affected by different clay types, tempers, and firing temperatures may provide important information for understanding this retention process. The formation of precipitates in the ceramic matrix from the reaction of fatty acids with calcium has been suggested as a possible mechanism that enhances lipid preservation (Hammann et al., 2020). Calcified deposits on the interior surfaces of archaeological pottery have also been related to the preservation of food-related proteins and substantial quantities of lipids (Hendy et al., 2018). The importance of chemical processes for the preservation of organic residues is widely known. The impact of physical characteristics of pottery on the retention of organic compounds, however, has been investigated to a significantly lesser extent. Porosity, the main such characteristic, is a widely diverse physical characteristic that depends on the raw materials and the manufacturing procedure. It has been investigated little in relation to organic products trapped within pottery walls (Drieu et al., 2019). A pottery material can have pores of various shapes, and the pores may be open (connected) or closed (isolated). The International Union of Pure and Applied Chemistry (IUPAC) classifies pores by their size as micropores (width <2 nm), mesopores (width from 2 nm to 50 nm), and macropores (width >50 nm) (Sing et al., 1985).

For archaeological organic residue preservation, pores in pottery provide most of the capacity for absorption of compounds into the material during cooking and are eventually responsible for protecting them from the environmental conditions while the pottery is buried in the ground (Evershed, 2008b; Drieu et al., 2019). The nature of pores was implicated as the basis for having absorbed lipid residues in archaeological chlorite vessels (Namdar et al., 2009) and even in glazed ceramics (Pecci et al., 2016). Drieu et al. (2019) suggested that a relatively greater fraction of overall pore volume occurring as 'small pores' (<1 μm) and overall porosity between 18 and 30% seemed to preserve the highest quantity of lipids in a ceramic matrix. Molecules inside micropores are less accessible to microorganisms and their extracellular enzymes, and are hence better protected from various burial-environment factors (Evershed, 2008b). The limited information on micro- and mesopore structures, amounts, and size distributions in archaeological pottery and on their fundamental role in the preservation of organic residues makes these pore properties an attractive target for a more thorough investigation.

To probe the micro- and mesopores (pores with widths <50 nm) associated with the different clay types, tempers, and firing temperatures used to produce archaeological pottery, the nitrogen (N_2) gas adsorption method was employed in the present study. A set of briquettes was made under controlled laboratory conditions to mimic the variability of materials and conditions used to manufacture primitive archaeological pottery. Briquettes of varying clay-temper ratio from each possible combination of two different raw clays (one illitic and one kaolinitic), two different tempers (quartz sand and chalk), and two different firing temperatures (600 and 800°C) were produced. In contrast to a set of archaeological pottery fragments, which may be limited to a particular clay type available to the manufacturer, the experimental briquettes in this study provide a good model to investigate a wide range of variability between clay and temper types and amounts. All the briquettes were subjected to quantitative X-ray diffraction (XRD) analysis. The findings revealed the effects of different materials and conditions on the ceramics' mineralogical composition and micro- and mesoporosity, providing, for the first time, a quantitative description of the micro- and mesopores in ceramics that mimic archaeological samples. The data from the set of briquettes created may become valuable as reference points for future mineralogy and porosity studies related to organic residue analysis.

Materials and methods

Preparation of briquettes

The reference pottery briquettes produced were intended to cover the characteristics of different archeological pottery types from the eastern Baltics (Kriiska, 1996; Tvauri, 2005; Dumpe et al., 2011; Kriiska et al., 2017). Two different clays were used as raw materials; first, a red clay in which illite and mixed-layered illite-smectite (I-S) are dominant, collected from a natural Quaternary clay formation in southeastern Estonia (near Joosu manor); and second, a white, kaolinite-rich clay obtained commercially (Bang & Bonsomer Group Oy, Helsinki, Finland) in powdered form. Although pure kaolinite was usually not the clay fabric in ancient pottery production, the inclusion of this raw clay variety in the study provided a generalized comparison of its porosity behavior relative to the illitic clay. For convenience, the red illitic clay is herein designated RC, and the white kaolinitic clay as WC. Shell debris, often found as temper in archaeological pottery in the eastern Baltics, was represented in this study by adding commercial powdered chalk (Bang & Bonsomer Group Oy, Helsinki, Finland) and is labeled as CH. Natural Quaternary sand, labeled as S, collected from Toome Hill in Tartu, Estonia, was used as sand temper. Because the sand was ungraded, it was sieved on a 0.500 mm mesh screen (no. 35 US Standard Mesh Number) and the finer fraction was mixed with the clays. Sieving was done to make the sand grain size uniform across every briquette. Forty individual mixtures of clay and temper, each 30.0 g in total, were prepared in briquettes (Table 1), each mixed by hand after weighing (B154-S, Mettler Toledo, OH, USA) the components. The clay-temper ratios were designed to cover the ranges of material combinations probably used by ancient potters, as well as to allow the effect of individual temper concentrations on different amounts of clay to be studied.

Two briquettes were also prepared from each dry raw clay material (RC and WC), without any added temper. To make a briquette, about 8–10 mL of ultra-pure water (Milli-Q® Advantage A10 system, Merck Millipore, Darmstadt, Germany) was added to 30.0 g of dry clay or mixed clay and temper (Table 1), and the resulting paste was molded into rectangular forms usually 3.0–3.5 cm × 5.0–6.0 cm. The thickness ranged from 0.8 cm to 1.0 cm. Each clay briquette was air-dried for about 12 h at room temperature and then placed in a drying oven (MOV-112F, Sanyo, Osaka, Japan) for another 24 h at 105°C before firing.

Firing of briquettes

Two equivalent sets of reference pottery briquettes were fired separately at 600 and 800°C in a muffle furnace (KL-22, Kerako, Tallinn, Estonia) equipped with an electronic programmable controller (ST315A, Stafford Instruments, Stafford, UK). The briquettes were fired in an oxidizing environment as follows: equilibrated at room temperature for 10 min, ramped to the desired final temperature (i.e. 600 or 800°C) within 1.5 h, and soaked at the target temperature for another 2 h. The briquettes were then left to cool to room temperature before they were removed from the muffle furnace and stored (Fig. 1).

https://doi.org/10.1017/cmn.2024.18 Published online by Cambridge University Press

Table 1. Mass fractions of clay and sand/chalk tempers used in making the reference pottery briquettes

Clay with sand temper			
Sample codes		Temper	
RC series	WC series	Clay	Sand (S)
RC600–S1, RC800–S1	WC600–S1, WC800–S1	15%	85%
RC600–S2, RC800–S2	WC600–S2, WC800–S2	20%	80%
RC600–S3, RC800–S3	WC600–S3, WC800–S3	25%	75%
RC600–S4, RC800–S4	WC600–S4, WC800–S4	50%	50%
RC600–S5, RC800–S5	WC600–S5, WC800–S5	75%	25%
RC600–S6, RC800–S6	WC600–S6, WC800–S6	100%	0%

Clay with sand and chalk tempers				
Sample codes		Temper		
RC series	WC series	Clay	Sand (S)	Chalk (CH)
RC600–CH1, RC800–CH1	WC600–CH1, WC800–CH1	20%	32%	48%
RC600–CH2, RC800–CH2	WC600–CH2, WC800–CH2	25%	30%	45%
RC600–CH3, RC800–CH3	WC600–CH3, WC800–CH3	50%	20%	30%
RC600–CH4, RC800–CH4	WC600–CH4, WC800–CH4	75%	10%	15%
RC600–CH5, RC800–CH5	WC600–CH5, WC800–CH5	90%	5%	5%

The values 600 and 800 in the sample codes refer to the firing temperatures of 600°C and 800°C.

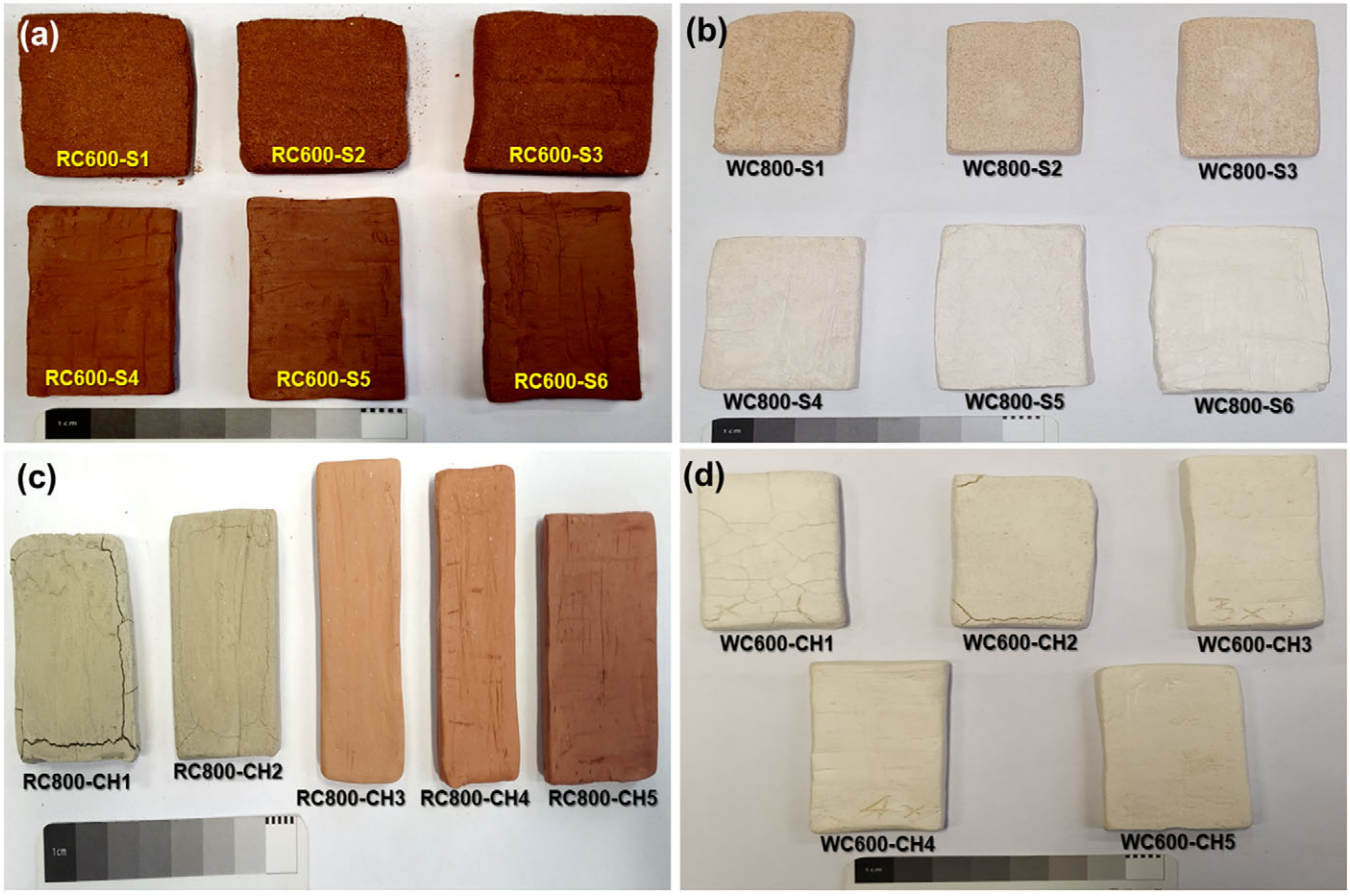

Figure 1. Photographs of some of the reference pottery briquettes composed of (a) illite and I-S (RC) with sand temper fired at 600°C, (b) kaolinite (WC) with sand temper fired at 800°C, (c) illite and I-S (RC) with chalk temper fired at 800°C, and (d) kaolinite (WC) with chalk temper fired at 600°C.

https://doi.org/10.1017/cmn.2024.18 Published online by Cambridge University Press

Analysis by X-ray diffraction

The mineralogical compositions of the 44 fired briquettes and the unfired raw materials (RC, WC, S, and CH) were obtained using a Bruker D8 Advance (Germany) X-ray diffractometer. Samples from the fired briquettes and unfired raw materials were dried for 24 h at 105°C, then pulverized using an agate mortar and pestle into fine powder. Three separate portions of each raw material powder and one portion of each fired-briquette powder were each transferred as unoriented powder into an aluminum sample holder and pressed with a glass slide to form a flat surface, which was then roughened with a razor blade. The measurements were done using Ni-filtered CuKα radiation in the range 3–70°2θ. For the identification of clay minerals, the clay fractions (<2 μm) of WC and RC were separated using standard procedures. The glass slide method was used to obtain oriented clay preparations in air-dried, ethylene glycol-solvated, and heated (to 550°C for 4 h) states. XRD data of the clay fractions were obtained within the 2–50°2θ. The quantitative and qualitative results were interpreted and modeled using a Rietveld algorithm-based code, Siroquant-3 software (Taylor, 1991).

Porosity analysis by nitrogen (N_2) gas adsorption

Pieces of the fired briquettes and samples of unfired raw materials, each weighing about 1.0 g, were placed in a 12 mm diameter round-bottomed glass sample holder and degassed at 300°C under vacuum for about 24 h using a sample degas system (VacPrep 061, Micromeritics, Norcross, GA, USA) to remove any moisture and other adsorbed species. N_2 adsorption on the degassed briquettes at varying relative pressure was measured with an adsorption analyser (3Flex, Micromeritics, Norcross, GA, USA). The total specific surface area (S_{BET}) was calculated according to the Brunauer–Emmett–Teller (BET) method (Thommes et al., 2015) from the amount of N_2 adsorbed in the $p/p°$ range from 0.05 to 0.2. An approximate value for the total specific volume of micro- and mesopores ($V_{0.95}$) was calculated from the amount of adsorbed N_2 at $p/p°$=0.95, which corresponds to the filling of pores with widths up to 41 nm based on the modified Kelvin equation applied for N_2 adsorbed at 77K in cylindrical pores (Lowell et al., 2004, table 8.1; Thommes et al., 2015).

The BET method can yield misrepresentative results for some materials (Sing, 2001). Therefore, to obtain a description of the porosity from the N_2 adsorption isotherms based on the specific structure present in clays, different non-local density functional theory (NLDFT) models for oxide materials with cylindrical pores were tested. These were applied to a series of repeated measurements of the RC600-S4 briquette, which had been made with 50% illitic clay and 50% sand, and was fired at 600°C (Appendix 1 in the Supplementary material). The NLDFT model for pillared clays (Olivier and Occelli, 2001) was found to be the most suitable for the investigated materials and was used in this study. The pore size distribution was calculated using this NLDFT model on the N_2 adsorption data with the 3Flex software (version 6.01, Micromeritics, Norcross, GA, USA). From the pore size distribution calculated with the NLDFT model, cumulative values for specific surface area (S_{NLDFT}) and specific pore volume (V_{NLDFT}) were obtained for pores with widths of up to 35 nm. Corresponding relative values of these parameters for micropores (under 2 nm) only, S_{micro} and V_{micro}, were also acquired and expressed as percentages. Appendix 2 in the Supplementary material addresses how well values of S_{NLDFT} and V_{NLDFT} compare with S_{BET} and $V_{0.95}$.

Results and Discussion

XRD analysis

Mineralogy of raw clays and tempers

Typical clay and non-clay minerals in unfired RC and WC were identified from the XRD patterns of randomly oriented whole-rock powders and oriented clay preparations (Fig. 2). Quantitative XRD analysis of the whole-rock powders showed that phyllosilicates were more abundant than other mineral phases in the two clays (see Table S1 in the Supplementary material). The dominant clay minerals in RC were the 2:1 phyllosilicate group (about 50 wt.% in total), which includes illite, I-S, and mica. Kaolinite (about 14 wt. %) was also present in RC. Kaolinite was the most abundant mineral in WC (about 74 wt.%), and the 2:1 phases constituted about 18 wt. %. The corresponding total amounts of clay minerals were 64% in RC and 91% in WC. Quartz, K-feldspar, and hematite in RC were the major non-clay minerals found in the raw clays.

The composition of clay fractions of RC and WC (Fig. 2) agreed well with the whole-rock XRD results. The 2:1 phyllosilicates of RC were a mixture of illite, I-S, and mica that caused prominent peaks at 10.0, 4.98, and 3.32 Å. After solvation of the clay with ethylene glycol (EG), the peak at 10.0 Å was different in shape (steeper on the low-angle side and less steep on the high-angle side) and a small, broad peak was present at 12.0 Å. After the clay was heated to 550° C, the 10.0 Å peak was thinner and higher than that of the air-dried clay. These differences in the XRD patterns indicate the presence before heating of some expanded interlayers in I-S. Kaolinite was also detected in the RC clay fraction by the peaks at 7.18 Å and 3.57 Å, which disappeared upon heating to 550°C. The primary clay mineral in the WC clay fraction, kaolinite, was characterized by strong, narrow peaks at 7.18 Å and 3.57 Å, which were unaffected by EG but were gone after heating to 550°C. Such narrow peaks indicate relatively large crystallites typical of well-ordered kaolinite (Awad et al., 2018). Kaolinite was accompanied by illite, mica (peaks at 9.98, 5.00, and 3.32 Å), and a trace of smectite (peak at 16.9 Å in the EG pattern).

As for the tempers used in this work (Fig. 3; Table S1 in the Supplementary material), the sand (S) was mainly composed of quartz, K-feldspar, and plagioclase with minor phyllosilicate (<6 wt.%) and carbonate (<4 wt.%) phases. The chalk (CH) was almost pure calcite (99 wt.%) with a small (trace or near trace) amount of dolomite and a trace of quartz, so its $CaCO_3$ content was close to that of shells (Barros et al., 2009), for which it was substituting as a temper.

Mineralogy of fired briquettes

Firing at 600°C caused no apparent change in mineralogical composition except for the disappearance of the kaolinite crystalline phase initially present in the raw clay materials, RC and WC (Fig. 4). Kaolinite dehydroxylates between 450 and 550°C, transforming into the amorphous metakaolinite (Frost et al., 2003). Another notable mineral transformation was the decomposition of calcite in chalk, a process generally occurring between 700 and 850°C (Allegretta et al., 2015). The decomposition of both calcite and dolomite was evident from the significantly smaller amounts of these carbonates in briquettes fired at 800°C compared with corresponding briquettes fired at 600°C. Lime (CaO) and portlandite ($Ca(OH)_2$) were observed in samples of chalk-tempered briquettes fired at 800°C, with CaO resulting from the decomposition of $CaCO_3$. Some of the CaO likely bound with atmospheric water vapor, diffusing through the material's open pores, and was converted to $Ca(OH)_2$ (Allegretta et al., 2015).

https://doi.org/10.1017/cmn.2024.18 Published online by Cambridge University Press

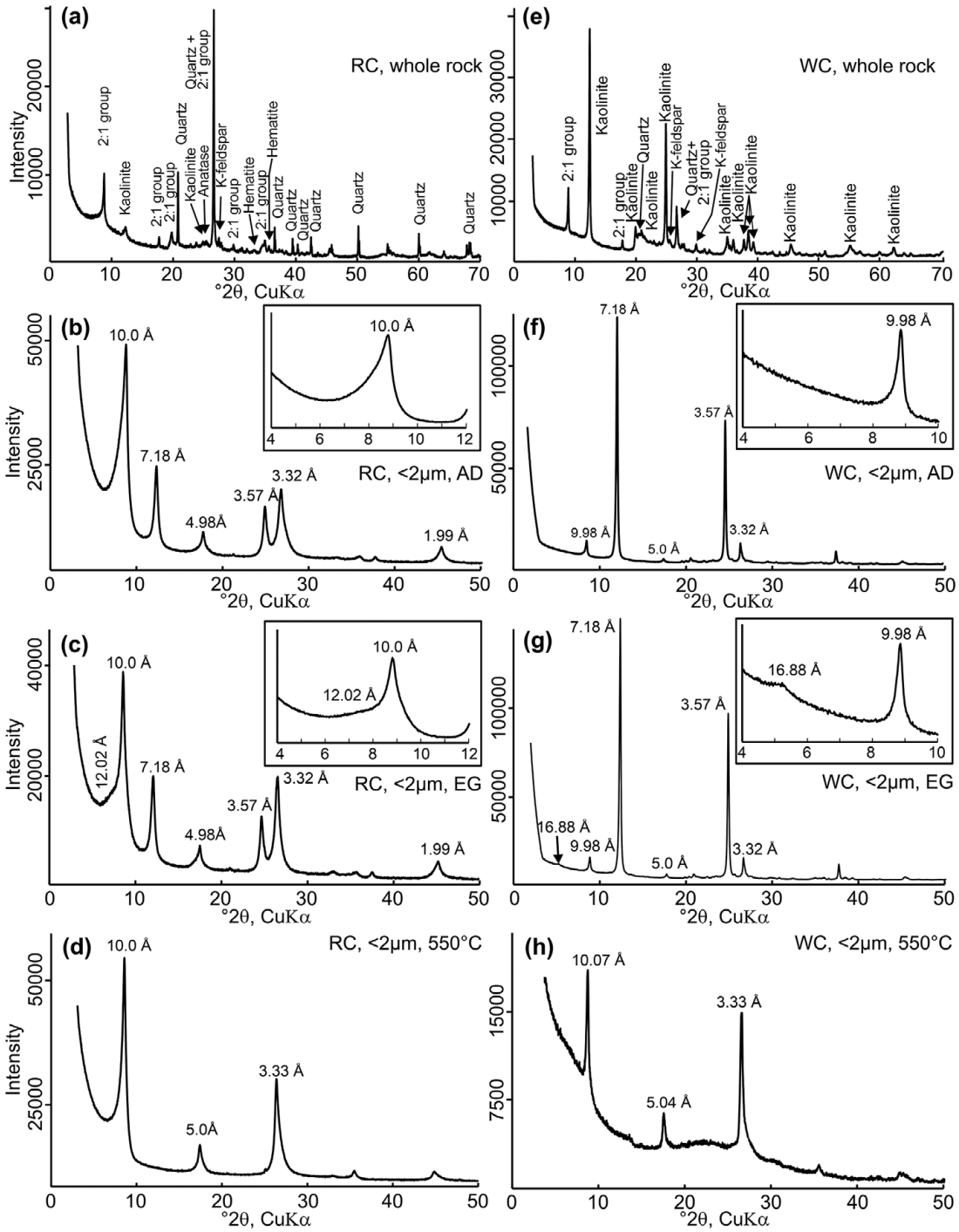

Figure 2. XRD patterns of the whole-rock raw clay materials composed mainly of (a) illite and I-S (RC), and (e) kaolinite (WC). Oriented clay preparation XRD patterns for RC and WC in air-dried (AD) (b and f), ethylene glycol-solvated (EG) (c and g), and heated to 550°C (d and h) forms.

Additionally, the high-temperature (800°C) reaction of clay minerals with lime induced the formation of calcium-silicate minerals (Allegretta et al., 2016). Larnite (Ca_2SiO_4) was found in all of the chalk-tempered briquettes fired at 800°C, and merwinite ($Ca_3Mg(SiO_4)_2$) was found in some of them. These products were more abundant in briquettes made with illitic clay than in briquettes made with kaolinitic clay. Brownmillerite, an oxide of calcium, aluminum, and iron that also forms through the reaction of lime with clay, was detected in only two chalk-tempered RC briquettes in amounts near the detection limit.

N_2 gas adsorption

Adsorption isotherms

Nitrogen adsorption isotherms show that the illitic clay raw material RC was much more adsorptive of N_2 than the kaolinitic clay WC (Fig. 5a). The sand (S) adsorbed very little N_2, which shows that micro- and mesoporosity are practically non-existent within it. The complex mineralogical nature of RC and WC, which are composed of mixtures of clay types based on XRD data, limits the physisorption isotherm type that can be assigned. The S-shaped

https://doi.org/10.1017/cmn.2024.18 Published online by Cambridge University Press

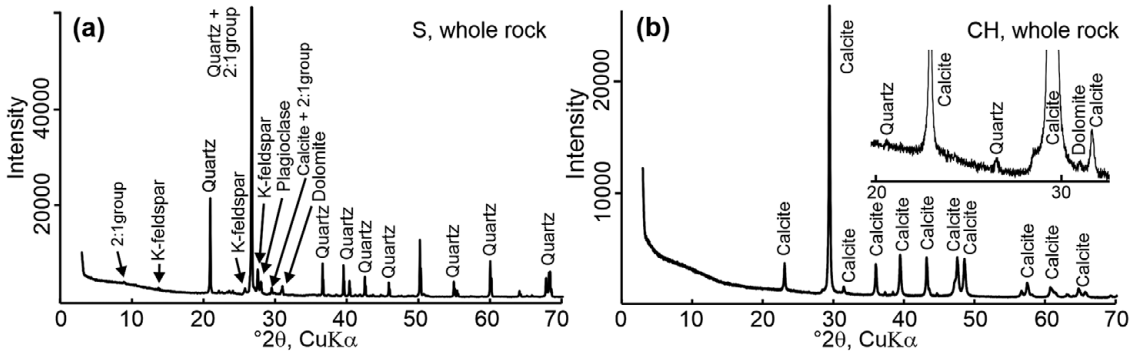

Figure 3. XRD patterns of the whole-rock temper raw material used in making briquettes: (a) sand (S), and (b) chalk (CH).

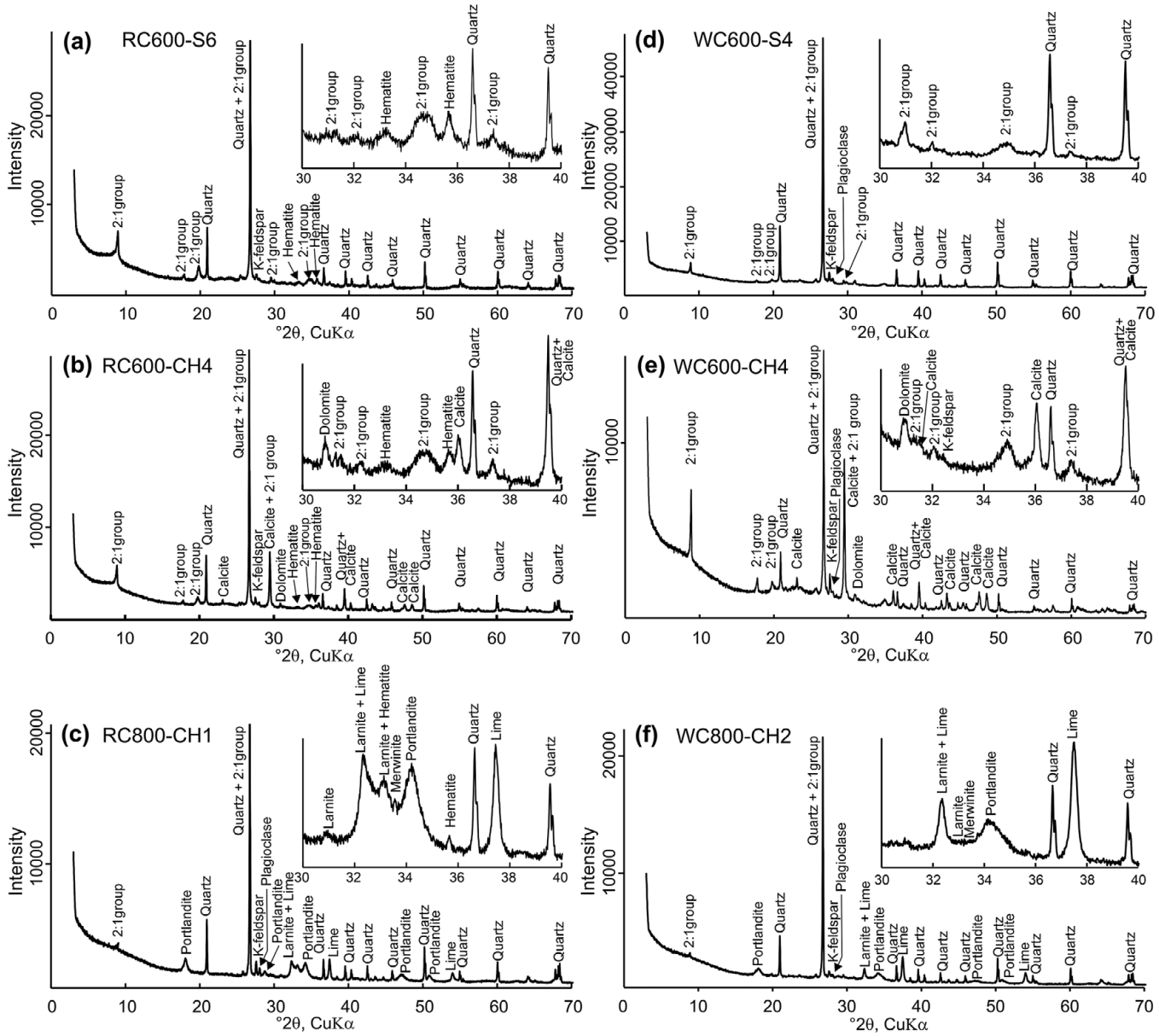

Figure 4. Representative XRD patterns of the RC (a to c) and WC (d to f) briquettes fired at 600 and 800°C.

https://doi.org/10.1017/cmn.2024.18 Published online by Cambridge University Press

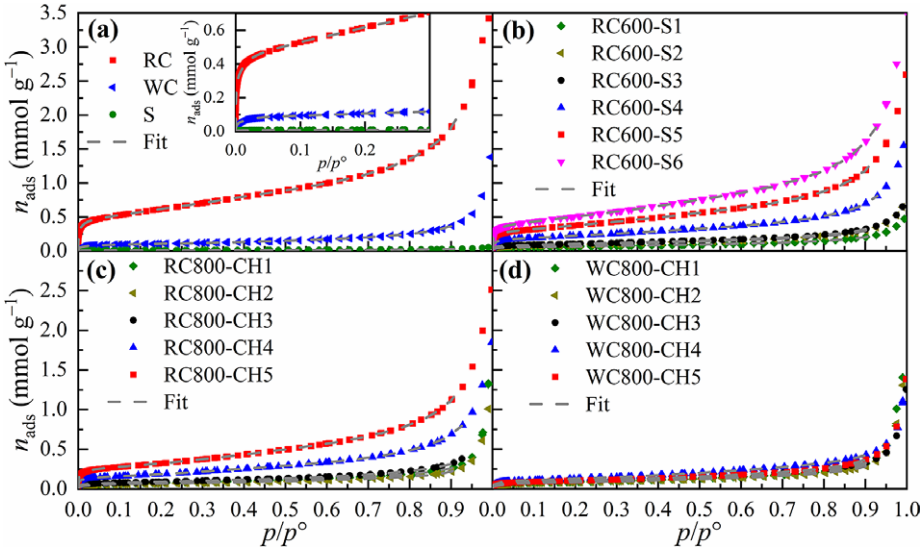

Figure 5. Nitrogen adsorption isotherms by adsorbed amount (n_{ads}) of N_2 on (a) the raw materials with a zoomed-in inset at lower $p/p°$ values, (b) the RC600-S series, (c) the RC800-CH series, and (d) the WC800-CH series with fits to the NLDFT model for pillared clays (dashed lines).

isotherms for RC and WC resemble those presented for Fithian illite and A.P.I.-5 kaolinite, respectively, by Aylmore (1974). Furthermore, the respective specific amounts of N_2 adsorbed by RC and WC were smaller than the amounts (converted from STP volumes) absorbed by the Fithian illite and A.P.I.-5 kaolinite, which is consistent with the observation that only about 50% of RC was illitic material and only about 74% of WC was kaolinite. The amounts of N_2 adsorbed by RC and WC at very low relative pressure ($p/p°$<0.01) also indicate substantial relative micropore volume in these clays. Firing the raw clays without temper (RC600-S6 and WC600-S6) did not cause a significant alteration in the shapes of the isotherms, but the amounts of N_2 adsorbed by RC were smaller after firing than before. The amount of N_2 adsorbed by the briquettes generally decreased as the amount of clay used to make them decreased (Fig. 5; Fig. S1 in the Supplementary material).

Pore characteristics of unfired source clays and sand

RC exhibited a greater specific surface area (S_{BET}) and overall specific micro- and mesopore volume ($V_{0.95}$) than WC (Table 2), implying that RC contains a more intricate network of open pores than WC. This is consistent with the XRD results that indicate relatively large, well-ordered crystallites of kaolinite in WC. S_{micro} and V_{micro} (Table 2) percentage values indicate a substantial presence of micropores in both of the raw clays. The contribution of micropores to the surface area is larger than their contribution to the pore volume.

Table 2. Surface area and pore volume parameters of raw materials determined from the N_2 adsorption isotherms

Raw material	Specific surface area			Specific pore volume		
	S_{BET} (m^2 g^{-1})	S_{NLDFT} (m^2 g^{-1})	S_{micro} (%)	$V_{0.95}$ (mm^3 g^{-1})	V_{NLDFT} (mm^3 g^{-1})	V_{micro} (%)
RC	50	62	57	87	68	17
WC	8.5	10.0	58	19	14	16
S	0.7	0.6	70	0.1	0.1	25

An extensive range of specific surface area values are reported in the literature for illite and I-S. For example, Dogan et al. (2007) reported values near 20 m^2 g^{-1} for the Silver Hill illite (special clays IMt-1 and IMt-2), while Aylmore et al. (1970) gave a value about ten times greater (195 m^2 g^{-1}) for the Willalooka soil illite. The 2:1 phyllosilicates of RC are a mixture of discrete illite, I-S, and mica, and the specific surface area for some well-known illitic clay types such as Fithian illite (Aylmore et al., 1970) and Morris illite (Aringhieri, 2004) are well within the 20–195 m^2 g^{-1} range, as is the reported value for RC. Illitic clays in a Quaternary clay deposit, such as RC, may have substantially different characteristics from the illitic clays used in most published literature. On the other hand, the surface area values of WC, which consists mostly of kaolinite, are within the range of values for well-ordered kaolinite reference samples (KGa-1 and KGa-1B source clays) of 8.4–11.7 m^2 g^{-1} reported by Pruett and Webb (1993). Comparison of values obtained in the present study to literature values is of limited worth because of the wide variability of different factors that affect the measured surface area. These factors are the degassing method, the grain size, and the clay composition, which includes layer charge and the nature of the exchangeable cations.

The surface area values for the sieved sand, both less than 1 m^2 g^{-1}, are consistent with a report by Ball et al. (1990) of less than 1 m^2 g^{-1} for medium- and fine-sand fractions of sandy aquifer material containing substantial amounts of K-feldspar and plagioclase. The very small surface area of S indicates that the 2:1 clay-mineral group in the sand (about 5% by mass) consists mainly of mica rather than the clay-sized illite or I-S.

Pore characteristics of fired briquettes

An RC briquette fired at 600°C without any temper additive (RC600-S6) had substantially smaller pore volume and surface area than the raw clay; $V_{0.95}$ decreased from 87 mm^3 g^{-1} in the unfired clay to 75 mm^3 g^{-1}, and S_{BET} decreased from 50 m^2 g^{-1} to 40 m^2 g^{-1} (Table 2; Table S2 in the Supplementary material). The observed differences in the micro- and mesoporosity between the raw RC and RC600-S6 are probably due to the manufacturing process of the fired briquette. The molding of the clay paste, which could have mechanically reduced porosity, and shrinkage

https://doi.org/10.1017/cmn.2024.18 Published online by Cambridge University Press

during drying of the wet paste and during firing may have contributed to this porosity reduction. No such differences between the fired clay and the raw clay were observed for WC. In fact, the specific porosity parameters of WC600-S6 were a little larger than those of the raw clay. These larger values, however, should not be attributed to porosity caused by firing. Specific parameters are relative to mass, so these larger values should be attributed to a substantial loss of mass (mostly as water vapor) during firing. In particular, the mass of the white clay was reduced by about 10% owing just to dehydroxylation of kaolinite.

The surface area and pore volume parameters of all the briquettes fired at 600°C are nearly proportional to the original clay content (Figs 6 and 7). Furthermore, the observed parameters of the WC600 briquettes are much smaller than those of the corresponding RC600 briquettes. These observations indicate that the clay in the briquettes fired at 600°C, although altered by heating, remained distinct from the temper and held virtually all of the micro- and mesoporosity.

All briquettes fired at 600°C and tempered with a combination of chalk and sand had smaller porosity parameters than corresponding briquettes tempered only with sand. For example, the S_{NLDFT} (31 $m^2\ g^{-1}$; Fig. 6) and the V_{NLDFT} (34 $mm^3\ g^{-1}$; Fig. 7) of chalk-tempered briquettes formed with 75% clay and fired at 600°C are lower than those of sand-tempered briquettes of corresponding clay content and firing temperature (35 $m^2\ g^{-1}$ and 40 $mm^3\ g^{-1}$, respectively). These differences can be attributed to the chalk causing an elevated pH of the water added to the clay paste during the manufacturing of the briquettes. Clay particles in a basic suspension are more easily disaggregated than those in an acidic suspension. Consequently, the basic aqueous solution within a paste containing powdered chalk should have promoted break-up of clay aggregates during briquette molding, leading to a reduction in intertactoid porosity.

The sand temper, consisting mainly (74 wt.%) of non-porous quartz that was unreactive during firing, had only a small effect on the pore parameters of sand-tempered briquettes fired at 800°C, in which clay was still the predominant contributor to porosity. Nevertheless, some small, systematic porosity differences are evident among the sand-tempered briquettes fired at the different temperatures (Figs 6 and 7). For example, the parameter values of the WC800-S briquettes are larger than the corresponding WC600-S values for the sand-rich compositions and smaller for the clay-rich compositions. These differences can be rationalized by examining two different processes occurring during heating at 800°C. First, decomposition of the small amount of dolomite in the sand temper (about 3%) to form porous magnesium and calcium oxides would have added to the porosity as long those oxides were not destroyed by reaction with clay. Second, sintering of the clay could have caused reduction in porosity (Msinjili et al., 2019). The first process would have had the greatest effect on the sand-rich WC800-S briquettes, while the second would have had the greatest effect on the clay-rich WC800-S briquettes. Hence, the sand-rich WC800-S briquettes exhibited larger porosity parameters than the corresponding WC600-S briquettes while the opposite was observed for the clay-rich briquettes. Most of the differences between the porosity parameters of the sand-tempered RC800 and RC600 briquettes are the same in sense and similar in magnitude to the differences between the corresponding pairs of sand-tempered WC briquettes. These differences between pairs of RC briquettes are very small, however, relative to the parameter values, which makes them less noticeable on the figures and more uncertain analytically than the corresponding differences among sand-tempered WC briquettes.

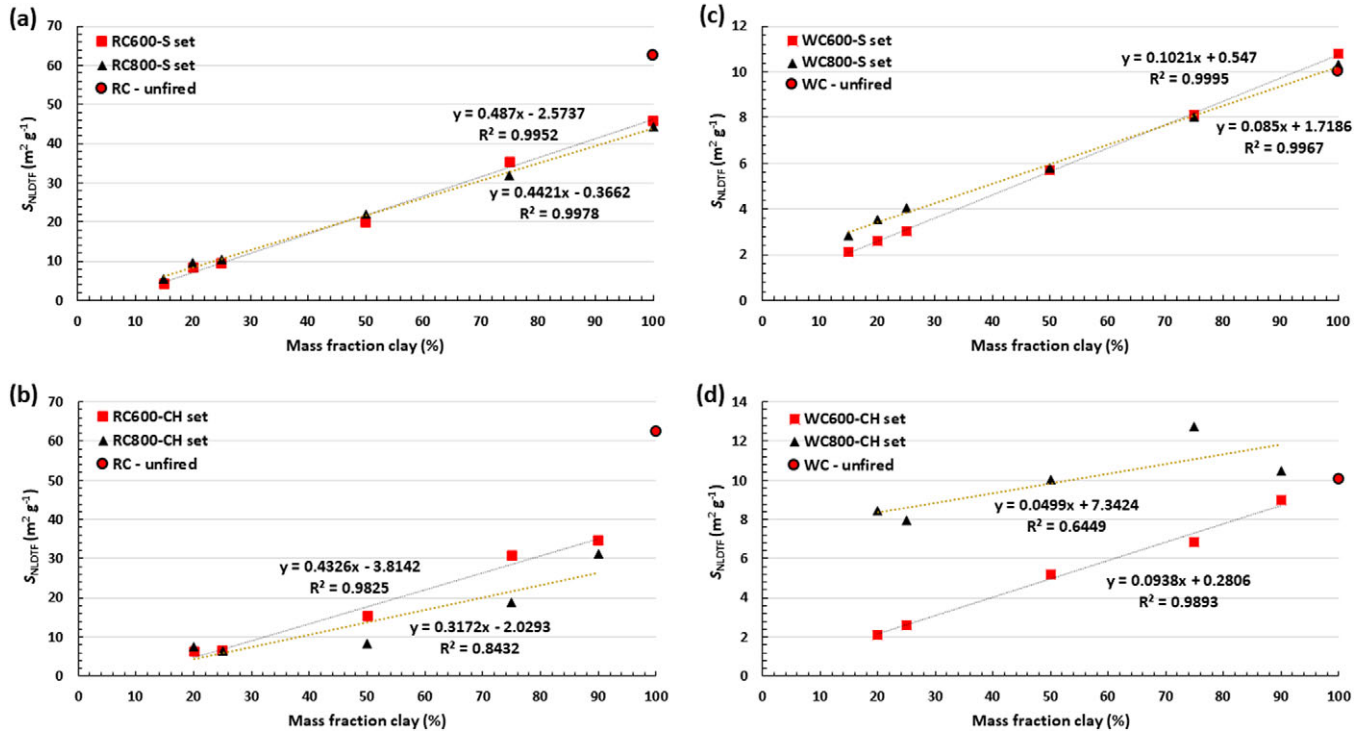

Figure 6. Graph of the specific surface area (S_{NLDFT}) *vs* the clay mass fraction (%) used to make the briquettes containing sand temper, within the set of RC (a) and the set of WC (c), and chalk temper, within the set of RC (b) and the set of WC (d).

https://doi.org/10.1017/cmn.2024.18 Published online by Cambridge University Press

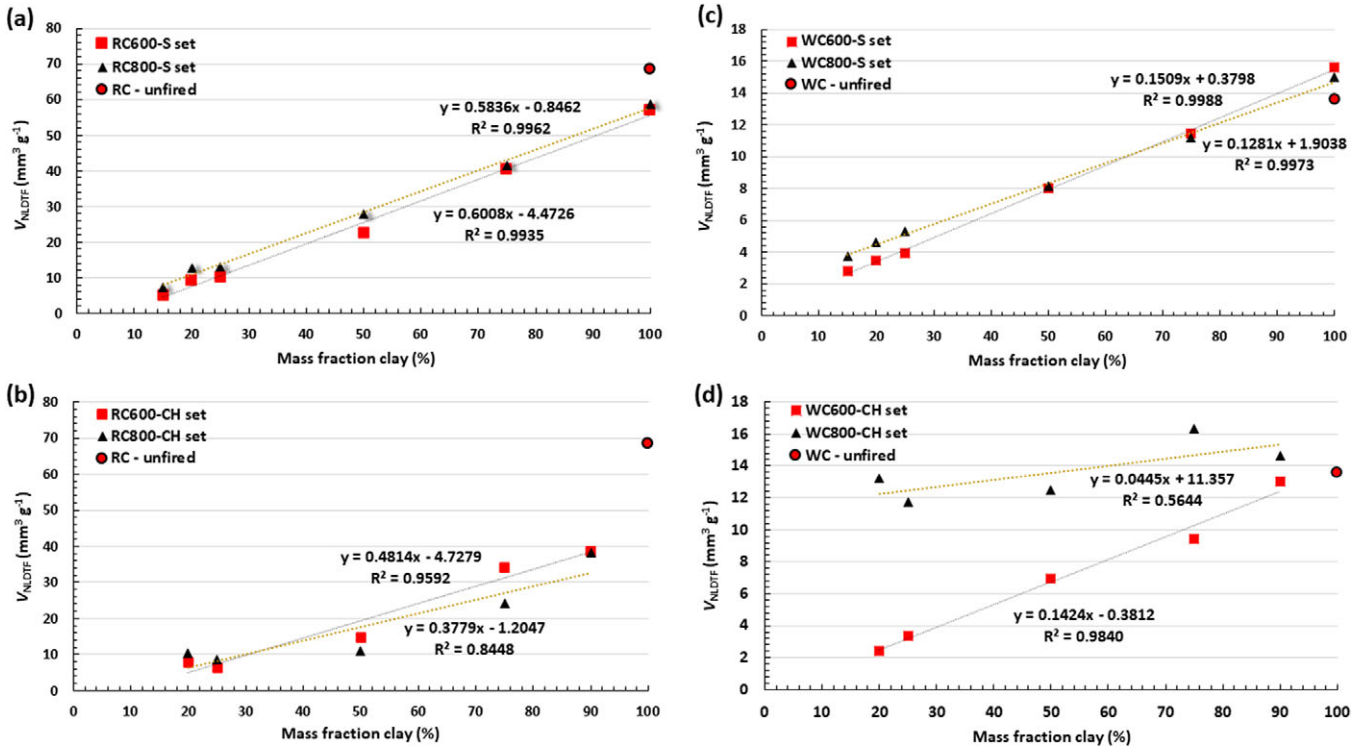

Figure 7. Graph of the specific pore volume (V_{NLDFT}) *vs* the clay mass fraction (%) used to make the briquettes containing sand temper, within the set of RC (a) and the set of WC (c), and chalk temper, within the set of RC (b) and the set of WC (d).

The pore parameters of some of the RC and WC chalk-tempered briquettes fired at 800°C were quite different from those of the corresponding briquettes fired at 600°C, causing noticeable deviations from the near proportionality of surface area and pore volume to the initial clay content. The effect of the higher firing temperature was pronounced in the WC chalk-tempered briquettes. Specifically, the parameter increases from the WC600-CH briquettes to the WC800-CH briquettes were substantially larger for the originally chalk-rich briquettes than for the clay-rich briquettes, causing a rapid divergence in parameter values between the WC800-CH briquettes and the WC600-CH briquettes with increasing original chalk content (Figs 6 and 7). The differences are roughly proportional to the amount of chalk added, suggesting that the additional observed porosity was in the solid decomposition products of the chalk, namely lime and portlandite. The loss of CO_2 from the calcite should have left behind highly porous lime. Some of this lime reacted with clay, forming presumably non-porous larnite and merwinite. However, the quantities of those reaction products are much less than and roughly proportional to the original amount of chalk added. Consequently, the amount of Ca in the remaining lime and post-firing mineral portlandite was less than, but approximately proportional to, the original amount of Ca in chalk. The observed increases in porosity due to higher temperature firing correlate well with the amounts of lime that remained in the WC800-CH briquette series as firing ended, some of which later became portlandite (see Table S1 in the Supplementary material).

The lime from decomposition of $CaCO_3$ during firing of chalk-tempered briquettes at 800°C affected the porosity of the material by reacting with clay. The much smaller porosity parameters of RC800-S3 and -S4 than the corresponding RC600 briquettes may be attributed to such reaction, which would have converted porous lime and porous clay to Ca silicates. These -S3 and -S4 briquettes originally had sufficient amounts of both clay and chalk for extensive reaction to be possible. Destruction of porosity by reaction of lime with the illitic clay appears to have been sufficient to outweigh the added porosity from lime that did not react. The nature of the clay minerals is undoubtedly the essential factor to consider in addressing the difference in the degree of reaction of CaO. If dehydroxylation made a clay mineral more susceptible to such reaction, one would expect that kaolinite should have reacted more with CaO than the illitic clay. However, mineralogical and porosity data indicate that the illitic clay reacted more extensively with CaO than the kaolinitic clay did. The finer grains of the illitic clay likely contributed to the more thorough reaction. Furthermore, illitic clay may have reacted more thoroughly with CaO due to its K and Na content. Kaolinite does not contain these alkali-metal oxides, which are well-known as effective fluxing agents (Msinjili et al., 2019).

Regardless of clay type and kind of temper, the fraction of microporosity (S_{micro} and V_{micro}) of the briquettes was smaller in the briquettes fired at 800°C than in those fired at 600°C. For instance, the chalk-tempered WC briquette with 25% clay content and fired at 600°C (WC600-CH2) exhibited an S_{micro} of 63% and a V_{micro} of 22%, which decreased to 51% and 14%, respectively, when the firing temperature was 800°C. The most prominent trend in microporosity fraction is that, for the sand-tempered briquettes, the differences generally were distinctly larger for the RC briquettes than for the WC briquettes. A possible reason for this microporosity difference is that sintering of illitic clay at 800°C, interpreted above as more extensive for RC than WC, reduced microporosity relatively more than mesoporosity. Distinct differences in microporosity fraction were also evident among the chalk-tempered briquettes fired at different

https://doi.org/10.1017/cmn.2024.18 Published online by Cambridge University Press

temperatures, where S_{micro} and V_{micro} were consistently smaller in the higher-temperature series. For the chalk-tempered briquettes made with kaolinitic clay, those difference are positively correlated with original chalk content. These observations are consistent with the evidence (described above) that most of the lime from calcite decomposition did not react with clay in the WC briquettes, and they indicate that the microporosity fractions were smaller in the lime (and perhaps in the later formed portlandite) than in the clay.

Pore-size distributions

The use of NLDFT models on heterogeneous and multi-component porous materials is not fully accurate and causes certain model-specific artifacts, such as a persistent minimum in pore-size distribution for pores with widths around 2 nm and a sharp peak for pores with a width of 5 nm. Despite these limitations in accuracy, the pore-size distributions obtained are precise in the sense that many of the comparisons between different raw materials and briquettes show good consistency. Examples of such consistency, seen in Figs 6 and 7, are (1) the very good correlations of porosity parameters to initial clay content in the cases where mineral reactions had only small effects on porosity and (2) the highly consistent differences of the parameter values for the three sand-rich RC briquette pairs and the three sand-rich WC pairs, where the differences were apparently due to a single process – formation of porous CaO and MgO by decomposition of a small amount of dolomite at 800°C.

Of the raw materials (Fig. 8), RC showed a bimodal distribution in the micropore range (<2 nm) with peaks at about 1.0 nm and 1.4 nm, while the WC distribution has only one peak in that range at around 1.5 nm. Bimodal pore-size distributions of illitic and kaolinitic clays in which the first peak was around 3 nm were reported by Kuila and Prasad (2013), but they were obtained with a calculation technique (the Barret, Joyner, and Halenda technique) that is not applicable to micropores. Hence, the results obtained for the micropore range in the present study, using the NLDFT model for pillared clays, cannot be compared with Kuila and Prasad's (2013) results. The much greater specific micropore volume of RC than WC is attributable to the effect of imperfect turbostratic stacking in tactoids of the illitic clay, as opposed to the more ordered stacking in kaolinite clays (Neaman et al., 2003), and also to generally smaller crystallites in illite than in kaolinite.

The pore-size distributions of all the sand-tempered briquettes were not significantly different in form from those of the respective raw clays (Fig. 9). The differential specific pore volumes of the briquettes of each series (that is, of the same clay type and firing temperature) varied in approximate proportion to the amount of clay used, and the differential volumes generally were slightly smaller in briquettes fired at 800°C than in corresponding ones fired at 600°C. These observations support the already expressed notions that the presence of sand had no large effect on the micro- and mesopores of the clay and that firing at 800°C was insufficient to cause extensive vitrification. The NLDFT-modeled pore-size distributions indicate that the volume of relatively large micropores (1–2 nm in width) was near 5 $mm^3\ g^{-1}$ for the RC600 and RC800 briquettes that had 75% clay initially. Thus, the briquettes perhaps most typical of the materials and conditions used to manufacture primitive archaeological pottery had a substantial volume of micropores. Such microporosity in ancient pottery should have been sufficient to hold and protect useful amounts of absorbed lipids.

The pore-size distributions of the chalk-tempered briquettes fired at 600°C also were not significantly different in form from those of the respective raw clays, but significantly different forms are apparent for those fired at 800°C (Fig. 10). A shift of the distribution maximum in the micropore region from around 1.4 or 1.5 nm to 1.7 nm was observed for five of the chalk-rich RC and WC briquettes fired at 800°C (i.e. RC800-CH1, -CH2, and -CH3 and WC800-CH1 and -CH2; -Fig. 10). Furthermore, the WC800-CH briquettes had greater micropore volume than the corresponding WC600-CH briquettes, and the more initial chalk, the greater the difference, relatively. This indicates that lime has substantial microporosity. On the other hand, among chalk-tempered RC briquettes, micropore volume was much smaller for the more strongly heated briquette of the two pairs (-CH3 and -CH4) that had enough of both clay and chalk for extensive reaction between the two to have occurred. This is consistent with the already presented evidence that the reaction with lime destroyed a substantial portion of the clay in most RC800-CH briquettes. The small amounts of clay remaining in originally chalk-rich RC800-CH1 and -CH2 (Table S1 in the Supplementary material) means that the microporosity of these briquettes, which peaks at 1.7 nm, was due mostly to unreacted lime.

A distinct change in form of the mesopore size distribution upon firing at 800°C was determined in the case of chalk-rich WC briquettes, where the volume of large mesopores (pores with widths >25 nm) was much greater than in corresponding briquettes fired at 600°C. These large differences were almost certainly due to lime that did not react with clay. They account for the distinctly smaller V_{micro} values in the chalk-rich WC800 briquettes than in corresponding WC600 briquettes, even though both micropore and mesopore volumes were larger in the WC800 briquettes. This supports the inference expressed above that the fractions of microporosity are smaller in the oxides formed by carbonate decomposition than in clay.

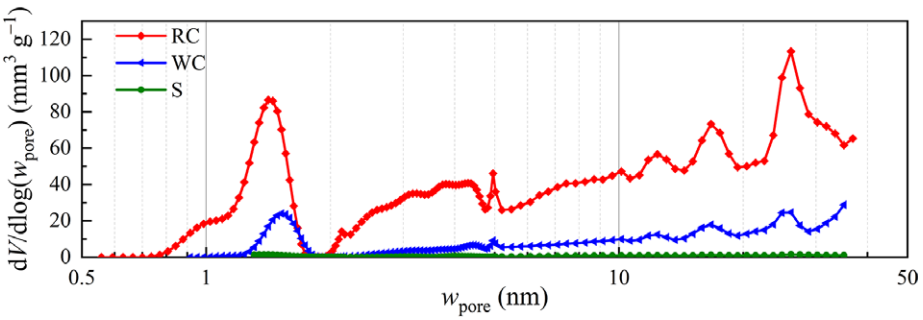

Figure 8. Pore-size distributions, as logarithmic differential pore volumes (dV/dlog(w_{pore})) *vs* pore widths (w_{pore}), of the RC, WC, and S raw materials obtained by application of the NLDFT model for pillared clays to the N_2 adsorption data.

https://doi.org/10.1017/cmn.2024.18 Published online by Cambridge University Press

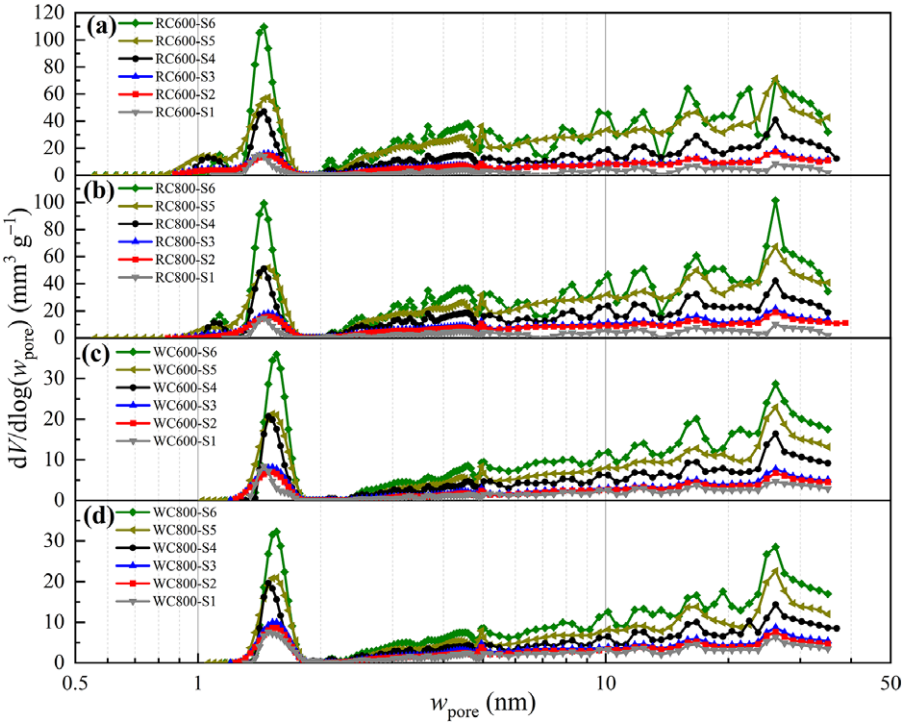

Figure 9. Pore-size distributions, as differential pore volumes (dV/dlog(w_{pore})) *vs* pore widths (w_{pore}), of samples of fired sand-tempered (and untempered) RC (a and b), and WC (c and d) briquettes obtained by application of the NLDFT model for pillared clays to the N_2 adsorption data.

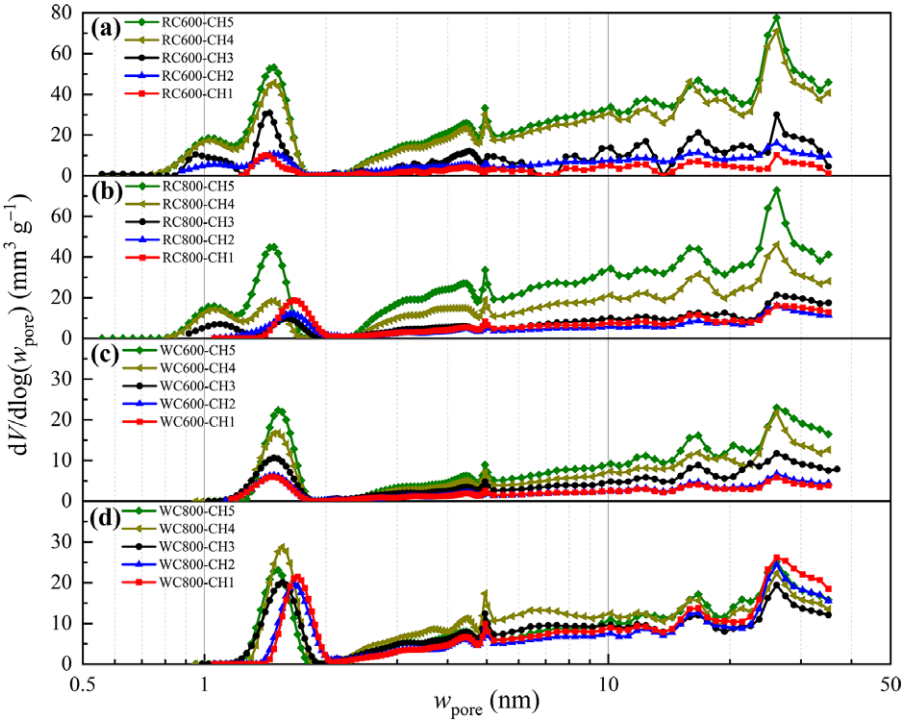

Figure 10. Pore-size distributions, as differential pore volumes (dV/dlog(w_{pore})) *vs* pore widths (w_{pore}), of samples of fired sand-and-chalk-tempered RC (a and b), and WC (c and d) briquettes obtained by application of the NLDFT model for pillared clays to the N_2 adsorption data.

Conclusions

A systematic study using X-ray diffraction and N_2 adsorption methods was conducted on clay briquettes that had been prepared from various combinations of illitic clay, kaolinitic clay, and sand and chalk tempers and were fired at temperatures of 600 and 800°C. Micro- and mesopore specific surface areas and specific pore volumes were largely dependent on the original porosity of the clay in the briquettes, as modified by mechanical porosity decreases

https://doi.org/10.1017/cmn.2024.18 Published online by Cambridge University Press

during molding, drying, and firing of the briquettes at 600°C and by mineralogical changes during firing at 800°C. These changes were influenced by the composition of added sand and chalk tempers. The elevated pH of chalk-bearing paste appears to have caused increased mechanical reduction of porosity in chalk-tempered briquettes. The presence of flux elements in illitic clay apparently contributed to sintering at 800°C. Clearly evident is that lime from decomposition of chalk reacted extensively with the illitic clay to greatly reduce micro- and mesoporosity in some of the briquettes. Conversely, lime formation in briquettes made with kaolinitic clay had an opposite effect on micro- and mesoporosity, because less extensive reaction of lime with kaolinite left the porosity of relatively large amounts of unreacted lime to be added to the original porosity. The sand temper was largely inert during firing, even at 800°C, but decomposition of a minor amount of dolomite in the sand appears to have added slightly to the porosity of the sand-rich briquettes fired at 800°C. For all fired briquettes, both micro- and mesoporosity were present, as evident from the pore size distributions. The relative contribution of microporosity in briquettes fired at the higher temperature of 800°C was smaller than in those fired at 600°C, but remained substantial, corresponding to micropore volumes around 5 $mm^3\ g^{-1}$ in some clay-rich briquettes.

The determined porosity characteristics of briquettes prepared from different clays, with different tempers, and fired at different temperatures provide valuable insights into the physical attributes of archaeological pottery in the micro- and mesopore regions. The amount and type of clay strongly influenced pore parameters, and so also did the presence of carbonate temper, especially for briquettes fired at 800°C. These observations and the information about micropore volumes offer insight for interpreting lipid residues from archaeological pottery. Given that pottery porosity is crucial for retaining organic biomolecules such as lipids, the findings in this study are relevant to future investigations on organic-residue analysis and have the potential to contribute to understanding differences in lipid preservation and yield from different pottery types.

Supplementary material. To view supplementary material for this article, please visit http://doi.org/10.1017/cmn.2024.18.

Author contributions. **Jan-Michael C. Cayme:** Conceptualization, Methodology, Formal analysis, Investigation, Writing-Original Draft, Writing-Review & Editing, Visualization; **Rasmus Palm:** Formal analysis, Writing-Review & Editing, Resources. **Peeter Somelar:** Formal analysis, Writing-Review & Editing, Resources; **Signe Vahur:** Writing-Review & Editing, Resources, Visualization, Supervision, Funding acquisition; **Ivo Leito:** Writing-Review & Editing, Resources, Visualization, Supervision, Funding acquisition; **Ester Oras:** Conceptualization, Writing-Review & Editing, Resources, Visualization, Supervision, Project administration, Funding acquisition.

Acknowledgements. This work was carried out using the instrumentation of the Estonian Centre of Analytical Chemistry (www.akki.ee). The authors acknowledge the critical reading, helpful insights, and the numerous suggestions of Professor Jesse Marion Wampler, which significantly improved this manuscript.

Financial support. This study was supported by the Estonian Research Council grants (PSG492 and PRG1198) and by the EU through the European Regional Development Fund (Centers of Excellence, TK141 'Advanced materials and high-technology devices for energy recuperation systems'). The Centers of Excellence effectively supports the gas adsorption instrumentation used for this study. E.O. was also supported by the Swedish Collegium for Advanced Study Pro Futura Scientia Fellowship.

Competing interests. The authors declare that they have no known competing financial interests or personal relationships that could have appeared to influence the work reported in this paper.

Data availability statement. The datasets generated from the interpretation of results are available. All the relevant data are included in the Supplementary material available in the online version of this article.

References

Allegretta, I., Eramo, G., Pinto, D., & Kilikoglou, V. (2015). Strength of kaolinite-based ceramics: comparison between limestone- and quartz-tempered bodies. *Applied Clay Science*, *116–117*, 220–230. https://doi.org/10.1016/j.clay.2015.03.018

Allegretta, I., Pinto, D., & Eramo, G. (2016). Effects of grain size on the reactivity of limestone temper in a kaolinitic clay. *Applied Clay Science*, *126*, 223–234. https://doi.org/10.1016/j.clay.2016.03.020

Aringhieri, R. (2004). Nanoporosity characteristics of some natural clay minerals and soils. *Clays and Clay Minerals*, *52*, 700–704. https://doi.org/10.1346/CCMN.2004.0520604

Awad, M. E., López-Galindo, A, Sánchez-Espejo, R., Sainz-Díaz, C. I., El-Rahmany, M. M., & Viseras, C. (2018). Crystallite size as a function of kaolinite structural order-disorder and kaolin chemical variability: sedimentological implication. *Applied Clay Science*, *162*, 261–267. https://doi.org/10.1016/j.clay.2018.06.027

Aylmore, L. A. G. (1974). Gas sorption in clay mineral systems. *Clays and Clay Minerals*, *22*, 175–183. https://doi.org/10.1346/CCMN.1974.0220205

Aylmore, L. A. G., Sills, I. D., & Quirk, J. P. (1970). Surface area of homoionic illite and montmorillonite clay minerals as measured by the sorption of nitrogen and carbon dioxide. *Clays and Clay Minerals*, *18*, 91–96. https://doi.org/10.1346/CCMN.1970.0180204

Ball, W. P., Buehler, C. H., Harmon, T. C., Mackay, D. M., & Roberts, P. V. (1990). Characterization of a sandy aquifer material at the grain scale. *Journal of Contaminant Hydrology*, *5*, 253–295. https://doi.org/10.1016/0169-7722(90)90040-N

Barros, M. C., Bello, P. M., Bao, M., & Torrado, J. J. (2009). From waste to commodity: Transforming shells into high purity calcium carbonate. *Journal of Cleaner Production*, *17*, 400–407. https://doi.org/10.1016/j.jclepro.2008.08.013

Courel, B., Robson, H. K., Lucquin, A., Dolbunova, E., Oras, E., Adamczak, K., Andersen, S. H., Astrup, P. M., Charniauski, M., Czekaj-Zastawny, A., Ezepenko, I., Hartz, S., Kabaciński, J., Kotula, A., Kukawka, S., Loze, I., Mazurkevich, A., Piezonka, H., Piličiauskas, G., Sørensen, S. A., Talbot, H. M., Tkachou, A., Tkachova, M., Wawrusiewicz, A., Meadows, J., Heron, C. P., and Craig, O. E. (2020). Organic residue analysis shows sub-regional patterns in the use of pottery by Northern European hunter-gatherers. *Royal Society Open Science*, *7*, 192016. https://doi.org/10.1098/rsos.192016

Daghmehchi, M., Rathossi, C., Omrani, H., Emami, M., & Rahbar, M. (2018). Mineralogical and thermal analysis of the Hellenistic ceramics from Laodicea Temple, Iran. *Applied Clay Science*, *162*, 146–154. https://doi.org/10.1016/j.clay.2018.06.007

Dogan, M., Dogan, A. U., Yesilyurt, F. I., Alaygut, D., Buckner, I., & Wurster, D. E. (2007). Baseline studies of the Clay Minerals Society special clays: specific surface area by the Brunauer Emmett Teller (BET) method. *Clays and Clay Minerals*, *55*, 534–541. https://doi.org/10.1346/CCMN.2007.0550508

Drieu, L., Horgnies, M., Binder, D., Pétrequin, P., Pétrequin, A.-M., Peche-Quilichini, K., Lachenal, T., & Regert, M. (2019). Influence of porosity on lipid preservation in the wall of archaeological pottery. *Archaeometry*, *61*, 1081–1096. https://doi.org/10.1111/arcm.12479

Dumpe, B., Bērziņš, V., & Stilborg, O. (2011). A dialogue across the Baltic on Narva and Ertebølle pottery. In S. Hartz, F. Lüth, & T. Terberger (eds), *Early pottery in the Baltic – dating, origin and social context* (pp. 409–442). Bericht der Römisch-Germanischen Kommission, Phillip von Zabern, Darmstadt/Mainz.

Evershed, R. P. (2008a). Organic residue analysis in archaeology: the archaeological biomarker revolution. *Archaeometry*, *50*, 895–924. https://doi.org/10.1111/j.1475-4754.2008.00446.x

Evershed, R. P. (2008b). Experimental approaches to the interpretation of absorbed organic residues in archaeological ceramics. *World Archaeology*, *40*, 26–47. https://doi.org/10.1080/00438240801889373

Evershed, R. P., Dudd, S. N., Copley, M. S., Berstan, R., Stott, A. W., Mottram, H., Buckley, S. A., & Crossman, Z. (2002). Chemistry of archaeological animal fats. *Accounts of Chemical Research*, *35*, 660–668. https://doi.org/10.1021/ar000200f

Evershed, R. P., Smith, G. D., Roffet-Salque, M., Timpson, A., Diekmann, Y., Lyon, M. S., Cramp, L. J. E., Casanova, E., Smyth, J., Whelton, H. L., Dunne, J., Brychova, V., Šoberl, L., Gerbault, P., Gillis, R. E., Heyd, V., Johnson, E., Kendall, I., Manning, K., Marciniak, A., Outram, A. K., Vigne, J.-D., Shennan, S., Bevan, A., College, S., Allason-Jones, L., Amkreutz, L., Anders, A., Arbogast, R.-M., Bălăşescu, A., Bánffy, E., Barclay, A., Behrens, A., Bogucki, P., Alonso, Á. C., Carretero, J. M., Cavanagh, N., Claßen, E., Giraldo, H. C., Conrad, M., Csengeri, P., Czerniak, L., Dębiec, M., Denaire, A., Domboróczki, L., Donald, C., Ebert, J., Evans, C., Francés-Negro, M., Gronenborn, D., Haack, F., Halle, M., Hamon, C., Hülshoff, R., Ilett, M., Iriarte, E., Jakucs, J., Jeunesse, C., Johnson, M., Jones, A. M., Karul, N., Kiosak, D., Kotova, N., Krause, R., Kretschmer, S., Krüger, M., Lefranc, P., Lelong, O., Lenneis, E., Logvin, A., Lüth, F., Marton, T., Marley, J., Mortimer, R., Oosterbeek, L., Oross, K., Pavúk, J., Pechtl, J., Pétrequin, P., Pollard, J., Pollard, R., Powlesland, D., Pyzel, J., Raczky, P., Richardson, A., Rowe, P., Rowland, S., Rowlandson, I., Saile, T., Sebők, K., Schier, W., Schmalfuß, G., Sharapova, S., Sharp, H., Sheridan, A., Shevnina, I., Sobkowiak-Tabaka, I., Stadler, P., Stäuble, H., Stobbe, A., Stojanovski, D., Tasić, N., van Wijk, I., Vostrovská, I., Vuković, J., Wolfram, S., Zeeb-Lanz, A., & Thomas, M. G. (2022). Dairying, disease and the evolution of lactase persistence in Europe. *Nature*, *608*, 336–345. https://doi.org/10.1038/s41586-022-05010-7

Frost, R. L., Horváth, E., Makó, É., Kristóf, J., & Rédey, Á. (2003). Slow transformation of mechanically dehydroxylated kaolinite to kaolinite – an aged mechanochemically activated formamide-intercalated kaolinite study. *Thermochimica Acta*, *408*, 103–113. https://doi.org/10.1016/S0040-6031(03)00316-2

Hammann, S., Scurr, D. J., Alexander, M. R., & Cramp, L. J. E. (2020). Mechanisms of lipid preservation in archaeological clay ceramics revealed by mass spectrometry imaging. *Proceedings of the National Academy of Sciences of the USA*, *117*, 14688–14693. https://doi.org/10.1073/pnas.1922445117

Hendy, J., Colonese, A. C., Franz, I., Fernandes, R., Fischer, R., Orton, D., Lucquin, A., Spindler, L., Anvari, J., Stroud, E., Biehl, P. F., Speller, C., Boivin, N., Mackie, M., Jersie-Christensen, R. R., Olsen, J. V., Collins, M. J., Craig, O. E., & Rosenstock, E. (2018). Ancient proteins from ceramic vessels at Çatalhöyük West reveal the hidden cuisine of early farmers. *Nature Communications*, *9*, 4064. https://doi.org/10.1038/s41467-018-06335-6

Kriiska, A. (1996). The Neolithic pottery manufacturing technique of the lower course of the Narva River. In T. Hackens, S. Hicks, V. Lang, U. Miller, & L. Saarse (eds), *Journal of the European Network of Scientific and Technical Cooperation for the Cultural Heritage. PACT 51. Coastal Estonia: Recent Advances in Environment and Cultural History*. Council of Europe (pp. 373–384). Rixensart, Belgium.

Kriiska, A., Oras, E., Lõugas, L., Meadows, J., Lucquin, A., & Craig, O. E. (2017). Late Mesolithic Narva stage in Estonia: pottery, settlement types and chronology. *Estonian Journal of Archaeology*, *21*, 52–86. https://doi.org/10.3176/arch.2017.1.03.

Kuila, U., & Prasad, M. (2013). Specific surface area and pore-size distribution in clays and shales. *Geophysical Prospecting*, *61*, 341–362. https://doi.org/10.1111/1365-2478.12028

Lowell, S., Shields, J. E., Thomas, M. A., & Thommes, M. (2004). *Characterization of Porous Solids and Powders: Surface Area, Pore Size and Density*. Springer, Dordrecht, Netherlands.

Lucquin, A., Robson, H. K., Eley, Y., Shoda, S., Veltcheva, D., Gibbs, K., Heron, C. P., Isaksson, S., Nishida, Y., Taniguchi, Y., Nakajima, S., Kobayashi, K., Jordan, P., Kaner, S., & Craig, O. E. (2018). The impact of environmental change on the use of early pottery by East Asian hunter-gatherers. *Proceedings of the National Academy of Sciences of the USA*, *115*, 7931–7936. https://doi.org/10.1073/pnas.1803782115

Mentesana, R., Kilikoglou, V., Todaro, S., & Day, P. M. (2019). Reconstructing change in firing technology during the final Neolithic-Early Bronze Age transition in Phaistos, Crete. Just the tip of the iceberg? *Archaeological and Anthropological Science*, *11*, 871–894. https://doi.org/10.1007/s12520-017-0572-8

Msinjili, N. S., Gluth, G. J. G., Sturm, P., Vogler, N., & Kühne, H.-C. (2019). Comparison of calcined illitic clays (brick clays) and low-grade kaolinitic clays as supplementary cementitious materials. *Materials and Structure*, *52*, 94. https://doi.org/10.1617/s11527-019-1393-2

Namdar, D., Stacey, R. J., & Simpson, S. J. (2009). First results on thermally induced porosity in chlorite cooking vessels from Merv (Turkmenistan) and implications for the formation and preservation of archaeological lipid residues. *Journal of Archaeological Science*, *36*, 2507–2516. https://doi.org/10.1016/j.jas.2009.07.003

Neaman, A., Pelletier, M., & Villieras, F. (2003). The effects of exchange cation, compression, heating and hydration on textural properties of bulk bentonite and its corresponding purified montmorillonite. *Applied Clay Science*, *22*, 153–168. https://doi.org/10.1016/S0169-1317(02)00146-1

Olivier, J. P., & Occelli, M. L. (2001). Surface area and microporosity of a pillared interlayered clay (PILC) from a hybrid density functional theory (DFT) method. *Journal of Physical Chemistry B*, *105*, 623–629. https://doi.org/10.1021/jp001822l

Oras, E., Lucquin, A., Lõugas, L., Tõrv, M., Kriiska, A., & Craig, O. E. (2017). The adoption of pottery by north-east European hunter-gatherers: evidence form lipid residue analysis. *Journal of Archaeological Science*, *78*, 112–119. https://doi.org/10.1016/j.jas.2016.11.010

Orton, C., & Hughes, M. (2013). *Pottery in Archaeology* (2nd edn). Cambridge University Press, UK.

Pecci, A., Degl'Innocenti, E., Giorgi, G., Ontiveros, M. A. C., Cantini, F., Potrony, E. S., Alós, C., & Miriello, D. (2016). Organic residue analysis of experimental, medieval, and post-medieval glazed ceramics. Archaeological and Anthropological Sci*ences*, *8*, 879–890. https://doi.org/10.1007/s12520-015-0262-3

Pruett, R. J., & Webb, H. L. (1993). Sampling and analysis of KGa-1B well-crystallized kaolin source clay. *Clays and Clay Minerals*, *41*, 514–519. https://doi.org/10.1346/CCMN.1993.0410411

Roffet-Salque, M., Regert, M., Evershed, R. P., Outram, A. K., Cramp, L. J. E., Decavallas, O., Dunne, J., Gerbault, P., Mileto, S., Mirabaud, S., Pääkkönen, M., Smyth, J., Šoberl, L., Whelton, H. L., Alday-Ruiz, A., Asplund, H., Bartkowiak, M., Bayer-Niemeier, E., Belhouchet, L., Bernardini, F., Budja, M., Cooney, G., Cubas, M., Danaher, E. M., Diniz, M., Domboróczki, L., Fabbri, C., González-Urquijo, J. E., Guilaine, J., Hachi, S., Hartwell, B. N., Hofmann, D., Hohle, I., Ibáñez, J. J., Karul, N., Kherbouche, F., Kiely, J., Kotsakis, K., Lueth, F., Mallory, J. P., Manen, C., Marciniak, A., Maurice-Chabard, B., Mc Gonigle, M. A., Mulazzani, S., Özdoğan, M., Perić, O. S., Perić, S. R., Petrasch, J., Pétrequin, A.-M., Pétrequin, P., Poensgen, U., Pollard, C. J., Poplin, F., Radi, G., Stadler, P., Stäuble, H., Tasić, N., Urem-Kotsou, D., Vuković, J. B., Walsh, F., Whittle, A., Wolfram, S., Zapata-Peña, L., & Zoughlami, J. (2015). Widespread exploitation of the honeybee by early Neolithic farmers. *Nature*, *527*, 226–230. https://doi.org/10.1038/nature15757

Roffet-Salque, M., Dunne, J., Altoft, D. T., Casanova, E., Cramp, L. J. E., Smyth, J., Whelton, H. L., & Evershed, R. P. (2017). From the inside out: upscaling organic residue analyses of archaeological ceramics. *Journal of Archaeological Science: Reports*, *16*, 627–640. https://doi.org/10.1016/j.jasrep.2016.04.005

Santacreu, D. A. (2014). *Materiality, Techniques and Society in Pottery Production: The Technological Study of Archaeological Ceramics Through Paste Analysis*. De Gruyter Open, Poland.

Seetha, D., & Velraj, G. (2015). Spectroscopic and statistical approach of archaeological artifacts recently excavated from Tamilnadu, South India. *Spectrochimica Acta Part A: Molecular and Biomolecular Spectroscopy*, *149*, 59–68. https://doi.org/10.1016/j.saa.2015.04.041

Sing, K. (2001). The use of nitrogen adsorption for the characterisation of porous materials. *Colloids and Surfaces A: Physicochemical and Engineering Aspects*, *187–188*, 3–9. https://doi.org/10.1016/S0927-7757(01)00612-4

Sing, K. S. W., Everett, D. H., Haul, R. A. W., Moscou, L., Pierotti, R. A., Rouquérol, J., & Siemieniewska, T. (1985). Reporting physisorption data for gas/solid systems with special reference to the determination of surface area and porosity (Recommendations 1984). *Pure and Applied Chemistry*, *57*, 603–619. https://doi.org/10.1351/pac198557040603

Taylor, J. C. (1991). Computer programs for standardless quantitative analysis of minerals using the full powder diffraction profile. *Powder Diffraction*, *6*, 2–9.

Thommes, M., Kaneko, K., Neimark, A. V., Olivier, J. P., Rodriguez-Reinoso, F., Rouquerol, J., & Sing, K. S. W. (2015). Physisorption of gases, with special reference to the evaluation of surface area and pore size distribution (IUPAC Technical Report). *Pure and Applied Chemistry*, *87* 1051–1069. https://doi.org/10.1515/pac-2014-1117

Tvauri, A. (2005). *Latest Iron Age Pottery in Estonia (from the 11th Century to the Middle of the 13th Century)*. Tartu-Tallinn, Estonia.

https://doi.org/10.1017/cmn.2024.18 Published online by Cambridge University Press